



Synthetic nuclear Skyrme matter in imbalanced Fermi superfluids with a multicomponent order parameter

Albert Samoilenka , Filipp N. Rybakov, and Egor Babaev
Department of Physics, KTH Royal Institute of Technology, 106 91 Stockholm, Sweden

 (Received 30 April 2019; published 13 January 2020)

Cooper-pair formation in a system of imbalanced fermions leads to the well-studied Fulde-Ferrell or Larkin-Ovchinnikov superfluid state. In the former case the system forms spontaneous phase gradients while in the latter case it forms a stripelike or a crystal-like density gradient. We show that in multicomponent imbalanced mixtures, the superfluid states can be very different from the Fulde-Ferrell-Larkin-Ovchinnikov states. The system generates gradients in both densities and phases by forming three-dimensional vortex-antivortex lattices or lattices of linked vortex loops. The solutions share some properties with the ostensibly unrelated Skyrme model of densely packed baryons and can be viewed as synthetic realization of nuclear Skyrme matter.

DOI: [10.1103/PhysRevA.101.013614](https://doi.org/10.1103/PhysRevA.101.013614)

I. INTRODUCTION

One of the most important examples of translation symmetry breaking in condensed-matter states is formation of a crystal of topological defects. In the simplest superconductors and superfluids, the topological defects originate from the fact that they are described by a complex field $\Psi = |\Psi|e^{i\theta}$, where the 2π -periodic field θ is called the superfluid phase. As a consequence, superfluid and superconducting vortices are characterized by one of the simplest topological indices, the integer phase winding N , which quantifies how many times the phase changes from 0 to 2π when one circumvents a vortex core. It is given by the line integral $N = \frac{1}{2\pi} \oint \nabla\theta \cdot d\mathbf{l}$. One of the state-defining properties of superfluids is that they form vortex lattices under rotation [1,2]. Superconductors form vortex lattices in an external magnetic field [3]. More recently, lattices of more complicated topological defects, skyrmions, became of paramount importance in magnetism [4]. The magnetic skyrmion is a two-dimensional texture of a dimensionless magnetization vector $\mathbf{m}(\mathbf{r})$ with a nonzero integer topological invariant given by the integral $q = \frac{1}{4\pi} \int \varepsilon_{abc} m_a \partial_x m_b \partial_y m_c dx dy$, where ε_{abc} is the Levi-Civita symbol. In films, both vortex and skyrmion lattices can be viewed as crystals of two-dimensional particlelike objects, while in three dimensions they can be viewed as lattices of stringlike objects. The consequences of spontaneous breakdown of translation symmetry dictate unique macroscopic responses of these condensed-matter systems such as transport, magnetic, and thermodynamic properties.

While two-dimensional lattices of topological defects are ubiquitous, the situation is very different in three dimensions. The most celebrated example where three-dimensional crystals of topological solitons were sought is the Skyrme model of nuclear matter [5–9]. This model was proposed to describe atomic nuclei as continuous particlelike solutions of the nonlinear field theory in three dimensions, in contrast to two-dimensional magnetic skyrmions.

The nuclear Skyrme model was originally defined in terms of an $SU(2)$ valued chiral field. Hence solutions can be characterized by a pair of complex fields Φ_1 and Φ_2

constrained by $|\Phi_1|^2 + |\Phi_2|^2 = 1$. Nuclear skyrmion solutions of this model are isolated particlelike states characterized by an integer topological charge (or index) Q , which is interpreted as a baryon number and is defined as the integral over the topological density

$$\rho_Q = \frac{1}{12\pi^2} \varepsilon_{abcd} \varphi_a \varepsilon_{ijk} (\partial_i \varphi_b \partial_j \varphi_c \partial_k \varphi_d), \quad (1)$$

where $\varphi_1 = \text{Re}(\Phi_1)$, $\varphi_2 = \text{Im}(\Phi_1)$, $\varphi_3 = \text{Re}(\Phi_2)$, and $\varphi_4 = \text{Im}(\Phi_2)$. If one associates vorticity with a complex field component, then the internal structure of the skyrmion can be interpreted as a bundle of linked closed vortex loops and the linking number corresponds to the value of the topological charge. Skyrmions with different topological charges belong to different homotopy classes and therefore cannot mutually transform into each other as a result of any perturbations. Particles with charges of the opposite sign attract each other and are annihilated, while those with the same sign form highly charged skyrmions with a morphology resembling Platonic solids [10]. As a consequence, it is expected that for an unlimited number of particles with charges of the same sign the ground state is a skyrmion crystal, that is, nuclear Skyrme matter [6–9]. Such solutions, although not realized in a terrestrial laboratory, give an important example of a three-dimensional crystal of topological defects, which has been hypothesized to share properties with nuclear matter in a neutron star.

The problem of spontaneous breakdown of translation symmetry in superfluid and superconducting states has been of great interest even without formation of topological defects. It takes place in Fulde-Ferrell-Larkin-Ovchinnikov (FFLO) states [11–15], which can be viewed as one of the first discussed examples of a supersolid state. They form in fermionic systems where there is a density imbalance of two species of fermions. As a consequence, Cooper pairing involves two fermions with momenta of different magnitude, ensuing from a periodic modulation of the phase or modulus of the order parameter. In the most general cases considered, the modulation of the order parameter is two or three dimensional [11–15]. In

the context of color superconductivity in dense quark matter, three-dimensional modulation is called a FFLO crystal [13]. Such crystalline order is associated with density modulation and is not characterized by topological indices, i.e., is not a lattice of topological defects. While in ultracold atoms the realization of a FFLO state in a three-dimensional parabolic trap was challenging, some of the challenges were removed by the invention of the box trap potential [16–18]. Furthermore, it was shown that FFLO-type solutions are much more robust near the box potential wall [19,20]. Furthermore, since often the phases which are fragile in single-component systems occupy a much larger domain in the multicomponent case, this raises the question of possible states in multicomponent imbalanced mixtures.

II. THE MODEL

In this paper we consider mixtures of two species of fermionic ultracold atoms. We consider the case where both spin populations are imbalanced. We show that, by contrast, in a two-component system, entirely different states arise. The system forms textures in the form of a three-dimensional lattice of nuclear skyrmions. This represents synthetic realization of the putative Skyrme nuclear matter.

The Ginzburg-Landau functional for the free-energy density of a single-component FFLO superfluid in the BCS limit of weak coupling was derived microscopically in [21]. Its two-component generalization can be written in dimensionless units as

$$\mathcal{F} = \sum_{a=1}^2 \{ \zeta_a |\Delta \Psi_a|^2 + K_a |\vec{\nabla} \Psi_a|^2 + \alpha_a |\Psi_a|^2 + \beta_a |\Psi_a|^4 + \xi_a (\text{Im}[\Psi_a^* \vec{\nabla} \Psi_a])^2 \} + \gamma |\Psi_1|^2 |\Psi_2|^2, \quad (2)$$

where $\Psi_1 = f_1 + if_2$ and $\Psi_2 = f_3 + if_4$ are a pair of complex order parameters, $\Psi_a = |\Psi_a| e^{i\theta_a}$. All the microscopic parameters of the model are absorbed in dimensionless coefficients $\zeta_{1,2}$, $K_{1,2}$, $\alpha_{1,2}$, $\beta_{1,2}$, and $\xi_{1,2}$. Microscopic derivation of the parameters in the single-component case [21] shows that all of them are of order unity (see the Appendix). Hence we performed the majority of the simulations for coefficients $\zeta_{1,2} = 1$, $K_{1,2} = -1$, $\alpha_{1,2} = -1$, $\beta_{1,2} = 1$, and $\xi_{1,2} = 1$. In cases where a different value was used, we give the corresponding number. The dimensionless unit of length corresponds to $\frac{\hbar v_F}{(\delta\mu)_{c2}}$, where v_F is the Fermi velocity and $(\delta\mu)_{c2}$ is the critical value for the chemical potential difference $\delta\mu = |\mu_\uparrow - \mu_\downarrow|$. In the two-component case one necessarily has to include an additional parameter γ that controls the strength of biquadratic coupling. In what follows we set $\gamma = 0.5$ so that the system is substantially far away from a phase separation regime.

The key feature of systems with FFLO-type instability is that for sufficiently large fermionic imbalance, the coefficient K for the gradient terms becomes negative. Therefore, the system forms gradients of the field in the ground state and those should be balanced by retaining positive terms arising at the next order with higher-order spatial derivatives. Note that a regime is also possible where the coefficient in front of the fourth-order potential term becomes negative and one should retain the sixth-order potential term. While in the recent microscopic Ginzburg-Landau derivation [21] the fourth-order

potential term does not change sign simultaneously with the second-order gradient term, we obtained stable solutions, of the kind discussed below, also in the model with the negative fourth- and positive sixth-order potential terms.

III. THE RESULTS

We investigate numerically stable states of the model (2) (for details see the Appendix). We find that these are three-dimensional crystals with the field configurations $\Psi_{1,2}(\mathbf{r})$ analogous to that for the pair $\Phi_{1,2}(\mathbf{r})$ in nuclear skyrmion crystals. Thus, the ultracold atomic multicomponent mixtures can exhibit the physical realization of a crystal of synthetic nuclear skyrmions. Remarkably, at the same time the state is an example of behavior of vortex matter being a crystal of linked closed vortex loops [see Fig. 1(a)].

In the solutions that we find the energy density is nonuniform and it breaks translation symmetry down to a three-dimensional crystal-like lattice. A typical unit cell of size $\lambda_{x,y,z}$ for the solutions we found is shown in Fig. 1(a). Isosurfaces corresponding to a constant value of the density of the first condensate ($|\Psi_1| = \text{const}$) represent a set of horizontal surfaces with an array of holes. Since it resembles several layers of the Swedish bread knäckebröd, for brevity we will call it the knäckebröd phase. While $|\Psi_2| = \text{const}$ isosurfaces are vertical cylinders passing through the knäckebröd holes. The phase winding of θ_2 is equal to $\pm 2\pi$ around each such cylinder and the plus and minus signs alternate in a checkerboard pattern. The phase θ_1 has $\pm 2\pi$ winding along the cross sections of the knäckebröd layer. Thereby, the second component forms a lattice of vortex and antivortex lines. If one considers the structure of only the second component, its cross section is, in some respects, similar to the spontaneous vortex-antivortex lattice in a two-dimensional imbalanced chiral superconductor [22].

Now we establish the relationship between this solution and the nuclear skyrmion crystal. The important fact about the states that we find is that they do not contain points or domains in which both order parameters are simultaneously zero. In this regard, the topological density (1) can be calculated by assuming $\varphi_i = f_i / \sqrt{\sum_{j=1}^4 f_j^2}$. Thereby, the integral over the density (1) in both models gives the same index Q , also known as the skyrmion number. Hence, we use the terms skyrmion, antiskyrmion, half-skyrmion, and quarter-skyrmion to denote cases when Q is 1, -1 , $1/2$, and $1/4$, respectively. Obviously, in contrast to the mathematically idealized nuclear Skyrme model, in the model under consideration the total index Q is not an absolute invariant. The remarkable fact about the states of a multicomponent imbalanced mixture that we find is that Q does not change, unless perturbations are sufficiently strong. Hence it provides an important quantitative characteristic revealing the relationship with the nuclear skyrmions.

The total skyrmion number Q for the unit cell presented in Fig. 1(a) is 4. This total Q is composed of skyrmion numbers of each individual node: positions with maxima of topological density (1). When counting the nodes marked in orange in Fig. 1(a), it is necessary to take into account that the same node may have several images due to periodic boundary conditions. Thus, we obtain that each node has $Q = 1/2$ and hence is represented by a half-skyrmion.

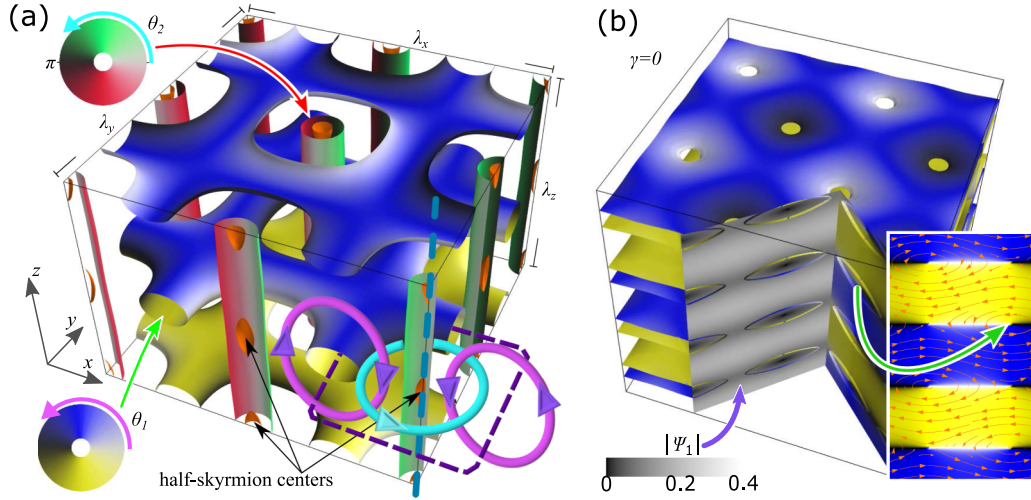


FIG. 1. Synthetic nuclear skyrmion crystal state in a mixture of imbalanced fermionic superfluids with two-component order parameter. It can be viewed as a stable state of linked vortex loops in two complex fields. (a) Isosurfaces of the order parameter modulus for $|\Psi_{1,2}| = 0.5 \max[|\Psi_{1,2}(\mathbf{r})|]$ in a unit cell of the crystal. The colors of the isosurfaces show the values of the corresponding phases $\theta_{1,2}$ in accordance with colormaps in the inserted circles. Orange areas show the isosurfaces of topological density for $\rho_Q = 0.95 \max[\rho_Q(\mathbf{r})]$. The cyan vertical dashed curve denotes the position of one particular vortex core for the second condensate, $\Psi_2 = 0$. The violet dashed curve denotes the position of one particular vortex core for the first condensate, $\Psi_1 = 0$, which forms stable vortex loops. Thick circles show several separate closed loops, along which there is a 2π phase winding in the condensates: Cyan corresponds to $|\Psi_2| = \text{const}$ and magenta corresponds to $|\Psi_1| = \text{const}$. The equilibrium periods which were found are $\lambda_{x,y} = 17.5$ and $\lambda_z = 12.5$. Average energy density $\langle \mathcal{F}(\mathbf{r}) \rangle = -0.43$. The simulation was performed for $K_{1,2} = -0.9$. (b) Knackebrod state of uncoupled condensates. Isosurfaces and their coloring are the same as in (a). The left vertical side of the triangular cutout shows the density distribution of the condensate in a black and white color code. The inset shows the map of streamlines. The numerical calculation was performed for $\alpha_{1,2} = 0$.

Note that the unit cell has an internal symmetry and in fact consists of eight smaller rectangular cells which are identical in their energy density $\mathcal{F}(\mathbf{r})$ and topological index density $\rho_Q(\mathbf{r})$ distributions, but have different order parameter configurations. We will call these \mathcal{F} cells.

Let us consider the distribution of order parameters in the vicinity of one half-skyrmion highlighted by the rightmost black arrow. The vertical dashed line passing through the center of the half-skyrmion depicts the vortex core in the second component. This means that $\Psi_2 = 0$ along this line. The thick circle with an arrow denotes the path around which $\oint d\theta_2 = 2\pi$ while $|\Psi_2|$ and θ_1 remain constant. Similarly to that, two parallel thick circles show two loops around which $\oint d\theta_1 = \pm 2\pi$. Thus, closely spaced vortex loops are linked.

One of the vortex cores in the first component ($\Psi_1 = 0$) is depicted by dashed loop. Note that cores of the second and first components (dashed curves) are also linked, since the vertical line for the second component may be viewed as part of a closed loop of infinite size. Hence the phase found can be considered as a collection of linked loops. However, there is a subtlety: Vertical vortex lines are passing through every hole in the knackebrod, white and black. This reflects the fact that in the vicinity of points of linking we do not find compact skyrmions with $Q = 1$, but rather pairs of half-skyrmions. In other words, two adjacent holes of different color constitute one fractionalized $Q = 1$ skyrmion. This is an observation common for all solutions in the two-component fermionic model: The two complex fields form lattices consisting of skyrmions fractionalized in half-skyrmions and even quarter-skyrmions.

In the limit when the coupling between the components is negligible, or in the single-component case, naturally there are no linkings. To highlight the difference with the two-component case, such a solution is presented in Fig. 1(b), for $\gamma = 0$. The structure of the order parameter in the form of parallel knackebrod layers is stable and qualitatively has a structure similar to that in the two-component case.

Figure 1(a) presents a simple tetragonal (st) crystal. That is not the only possible state. We found a variety of solutions composed of half-skyrmions forming body-centered-tetragonal (bct) crystals. The family of stable states is depicted in Fig. 2. Let us classify these solutions according to their lattice type and morphology.

Generalization of the st solution appears when the system makes connections between vertical vortex lines of the second component. The stable solutions have these connections in the space between the knackebrod layers. Such solutions include twice as many layers in the elementary cell. The bct crystal shown in Fig. 2(a) remains stable over a much larger range of parameters than the st crystal. By stability we mean that the given crystal is protected by an energy barrier that prevents a spontaneous transition to another crystal, expansion or shrinking of the unit cell, and other transformations. For this state the index $Q = 8$ per elementary cell. Hence, each \mathcal{F} cell has $Q = 1$, which reflects the fact that this cell contains a pair of half-skyrmions.

A very different stable state that the system forms can be viewed as a twisted st skyrmion lattice. This phase corresponds to DNA-like configuration of vortices spanning the system shown in Fig. 2(c). It consists of elongated half-skyrmions and has an overall index $Q = 8$ per elementary cell.

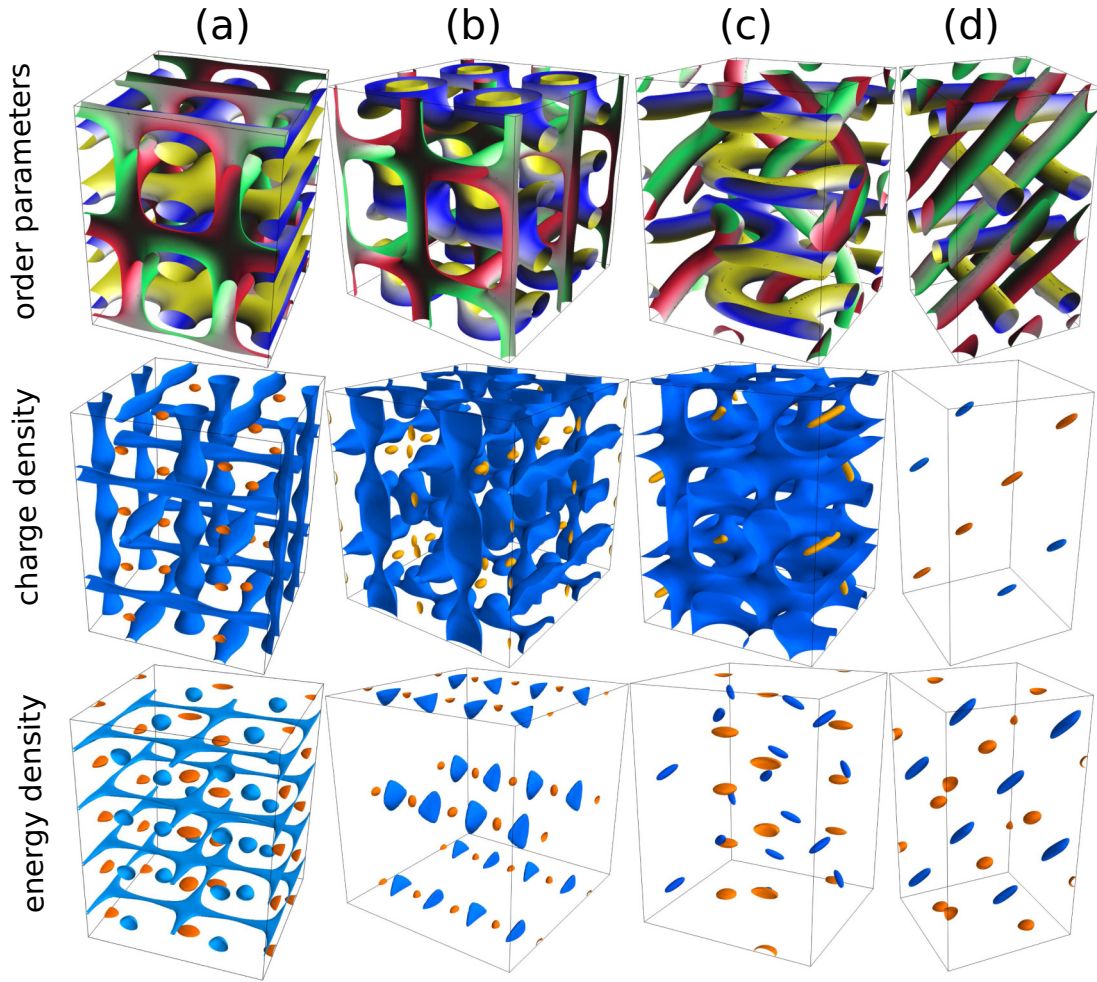


FIG. 2. Synthetic skyrmion crystals of different symmetries. The top row shows isosurfaces of the order parameter modulus for $|\Psi_{1,2}| = 0.5 \max[|\Psi_{1,2}(\mathbf{r})|]$; color encodes the values of corresponding phases $\theta_{1,2}$ as in Fig. 1(a). The middle row shows isosurfaces of the topological density: Orange corresponds to $\rho_Q = 0.95 \max[\rho_Q(\mathbf{r})]$ and blue corresponds to (a)–(c) $\rho_Q = 0.05 \max[\rho_Q(\mathbf{r})]$ and (d) $\rho_Q = -0.95 \max[\rho_Q(\mathbf{r})]$. The bottom row shows isosurfaces of the energy density: blue corresponds to $\mathcal{F}(\mathbf{r}) = 0.95 \min[\mathcal{F}(\mathbf{r})]$ and orange to $\mathcal{F}(\mathbf{r}) = 0.95 \max[\mathcal{F}(\mathbf{r})]$. (a) Unit cell of a bct lattice with equilibrium periods $\lambda_{x,y} = 15.1$ and $\lambda_z = 19.3$. The average energy density $\langle \mathcal{F}(\mathbf{r}) \rangle = -0.45$. (b) Different kind of stable bct lattice characterized by the fact that half-skyrmions are fractionalized into quarter-skyrmions, $\lambda_{x,z} = 21.0$, $\lambda_y = 19.5$, and $\langle \mathcal{F}(\mathbf{r}) \rangle = -0.44$. (c) DNA-like lattice characterized by the energy density $\langle \mathcal{F}(\mathbf{r}) \rangle = -0.46$, $\lambda_{x,y} = 15.7$, and $\lambda_z = 20.7$. For this solution the cores of half-skyrmions are noticeably elongated. (d) Skyrmion-antiskyrmion lattice with $\langle \mathcal{F}(\mathbf{r}) \rangle = -0.46$, $\lambda_{x,y} = 11.9$, and $\lambda_z = 21.9$.

The system can form a crystal with more complicated fractionalization, composed of quarter-skyrmions. In such a crystal there are reconnections that occur between layers of the knackebrod phase in the bct lattice. This gives chains of adjacent vortex loops [see Fig. 2(b)]. We term this crystal bct (chains) since it has skyrmion number $Q = 8$.

The synthetic nuclear Skyrme crystals presented above can be seen as a spontaneous formation of lattices of skyrmion fractions with the same Q . However, we found solutions for which the signs of the skyrmion number alternate. An example of a stable state with total skyrmion number $Q = 0$ is shown in Fig. 2(d). This state, which isosurface morphology superficially resembles the structure of blue phases in liquid crystals [23], has an equal number of skyrmions and anti-skyrmions, i.e., it can be interpreted as a particle-antiparticle crystal.

IV. CONCLUSIONS

The formation of a crystal of topological excitations, i.e., a vortex lattice, is considered a hallmark of superfluidity. A different kind of lattice of topological solitons was explored in the nuclear Skyrme model [5]. There, substantial effort was devoted to searching for solutions for nuclear skyrmion crystals that were hypothesized to describe matter in a neutron star, which led to an active research direction in mathematical physics [6–9]. An imbalanced Fermi superfluid is a seemingly unrelated system which is known to form a well-studied FFLO state. By performing a numerical energy minimization of the Ginzburg-Landau model we demonstrated that a multicomponent mixture of imbalanced superfluids has many stable states which are principally different from the FFLO state as well as from other known states such as Larkin-Ovchinnikov

crystals [13], an interior gap [24], and the Sarma phase [25], but is closely connected to the ostensibly unrelated Nuclear skyrmion crystals solutions [6–9]. The states exist in a range of parameters and do not require fine-tuning. In the states that we find nonlinear effects are highly important and the structure of the states cannot be captured by naive *ansatz*, but requires numerical solution of the full nonlinear problem. This calls for investigation into whether these states are relevant in the microscopically different physics arising in a dense QCD context [13,26]. These states carry a nontrivial density of topological index relating them to nuclear Skyrme crystals. Hence the system has spontaneous superflow in the form of a stable crystal of closed vortex loops. This means that in the system with negative gradient terms, the vortex-antivortex lattice is a very competitive solution. Note that such a configuration inherently has gradients in both the phases and densities of the fields.

Possible systems where nuclear Skyrme crystals may possibly be realized could be mixtures of ${}^6\text{Li}$ and ${}^{161}\text{Dy}$, ${}^{171}\text{Yb}$ and ${}^{173}\text{Yb}$, ${}^{161}\text{Dy}$ and ${}^{163}\text{Dy}$, ${}^6\text{Li}$ and ${}^{40}\text{K}$, and ${}^{40}\text{K} - {}^{161}\text{Dy}$ or mixtures involving ${}^{87}\text{Sr}$, ${}^{53}\text{Cr}$, and ${}^3\text{He}$. Fermi-Fermi mixtures were experimentally explored for ${}^6\text{Li}$ and ${}^{40}\text{K}$ [27,28]. Recently, the realization of a ${}^{40}\text{K} - {}^{161}\text{Dy}$ mixture was reported [29]. The mixtures considered have multiple stable states representing very different local minima. In order to make a crystal a global energy minimum, one may utilize the fact that their energy density is also a three-dimensional crystal, i.e., when one adds an external, periodic in all three directions, potential $U(\mathbf{r})|\Psi|^2$ these state can become a global minimum. Likewise, axion-type additional terms [30], which are proportional to the topological density (1), can make some of these states global minima, since skyrmion crystals with skyrmion numbers of the same sign can get a significant energy gain. Even when the skyrmion crystals represent local minima, upon cooling the system would likely form coexistent states or imperfect crystals, even in a box potential [16–18]. The direct route to create these crystals in experiments is via a relaxation from an imprinted similar configuration. There has been recent progress in imprinting nontrivial topological charges [31]. Because the skyrmion crystals can be viewed as a spontaneous lattice of vortex loops or lines, their experimental observation can be done via the same protocol as the observation of the ordinary vortex states. The other experimental route is the spectroscopy approach [32,33]. The nuclear Skyrme crystals that we find in the context of cold atoms can form in unconventional superconductors where multicomponent models are ubiquitous.

ACKNOWLEDGMENTS

We thank D. Weld, M. Zwierlein, A. Zyuzin, and W. Ketterle for useful discussions. We thank D. Weld and M. Zwierlein for pointing out the possible experimental realizations of imbalanced fermionic mixtures with multicomponent order parameter. The work was supported by the Swedish Research Council Grants No. 642-2013-7837, No. 2016-06122, and No. 2018-03659 and Göran Gustafsson Foundation for Research in Natural Sciences and Medicine and Olle Engkvists Stiftelse. Part of this work was performed at the Aspen Center for Physics,

which is supported by National Science Foundation under Grant No. PHY-1607611.

APPENDIX

1. Parameters

In the simplest single-component FFLO Ginzburg-Landau model [21], it is possible to rescale parameters so that all dimensional parameters are absorbed into α , which is a function of an imbalance of fermionic populations and temperature. To do so one should rescale $\mathcal{F} \rightarrow \frac{\epsilon_F}{n\Delta_{\text{BCS}}}\mathcal{F}$, $x \rightarrow \frac{1}{q_0}x$, and $\Psi \rightarrow \Delta_{\text{BCS}}\Psi$. Where, according to [21], $q_0 = \frac{1.81\Delta_{\text{BCS}}}{hv_F}$, $\Delta_{\text{BCS}} = \frac{h_{c2}}{0.754}$ and h_{c2} is a critical value for the chemical potential difference $h = \frac{1}{2}(\mu_{\uparrow} - \mu_{\downarrow})$. Next ϵ_F and v_F are the Fermi energy and velocity, respectively, and n is the density of particles. The rescaled energy density becomes

$$\mathcal{F} = \zeta|\Delta\Psi|^2 + K|\vec{\nabla}\Psi|^2 + \alpha|\Psi|^2 + \beta|\Psi|^4 + \xi(\text{Im}[\Psi^*\vec{\nabla}\Psi])^2, \quad (\text{A1})$$

with $\zeta = 0.61$, $K = -1.21$, $\alpha = 0.75 \ln(\frac{9h}{4h_{c2}})$, $\beta = 0.375$, and $\xi = 0.915$. Note that α can be positive or negative, depending on the ratio h/h_{c2} .

The two-component model necessarily has more parameters. We include the biquadratic coupling term $\gamma|\Psi_1|^2|\Psi_2|^2$. Apart from that, when rescaling space $x \rightarrow \lambda x$ and energy density $\mathcal{F} \rightarrow h\mathcal{F}$, we have to multiply by the same scaling factor for both components. This means that the model will depend on ratios of these factors for different components, namely, the space scaling factor for the first component will be proportional to $(\frac{h_{c2}}{v_F})_1(\frac{v_F}{h_{c2}})_2$, where indices correspond to the first and second components. Similarly for the energy scaling, we obtain the factor $(\frac{nh_{c2}^2}{\epsilon_F})_1(\frac{\epsilon_F}{nh_{c2}^2})_2$.

In the mixtures of two species of fermionic ultracold atoms characteristics like densities will be different. This means that in general we have $\zeta_1 \neq \zeta_2$, $K_1 \neq K_2$, etc. The disparity in these parameters leads to a tendency to improve the stability of the various crystal solutions. Hence we set all parameters to be equal in our computations to assess the system in a regime that is *less* favorable for crystal formation. We take all coefficients to be of order unity and set $K_1 = K_2 \simeq -1$, $\alpha_1 = \alpha_2 = -1$, $\gamma = 0.5$, and other parameters equal to unity.

2. Numerical algorithm

We numerically minimized the averaged energy density $\langle \mathcal{F} \rangle$ of the cuboidal unit cell of the full three-dimensional model [see Eq. (2)] with periodic boundary conditions and rescaling of all three spatial sizes λ_i of the cell independently. As a minimization routine we implemented the nonlinear conjugate gradient algorithm, parallelized on CUDA-enabled GPU. The domain was discretized by a mesh with 128^3 points. Some solutions were verified on the mesh with 256^3 points. In addition, we checked that the solutions remain stable on a relatively coarse grid with 64^3 points. The second-order finite-difference discretization scheme was applied to a continuous Hamiltonian [see Eq. (2)].

First of all, the solutions found provide a minimum of the energy for a single unit cell of fixed size, i.e., $E_0 = \int_0^{\lambda_x} \int_0^{\lambda_y} \int_0^{\lambda_z} \mathcal{F}(\mathbf{r}) dx dy dz \rightarrow \min$. Next the periods $\lambda_{x,y,z}$ are

in equilibrium, i.e., they are variables in the problem and were found such that simultaneously they provide a minimum for the average energy density, $\langle \mathcal{F}(\mathbf{r}) \rangle = E_0/\lambda_x\lambda_y\lambda_z \rightarrow \min$.

A similar approach, based on minimization of the average energy density, was used to study one-dimensional helicoidal ordering in magnets without an inversion center [34]. Subsequent experiments confirmed the phenomenon and the equilibrium periods on a quantitative level [35].

Because the system has many states representing local minima, to obtain a regular crystal one needs a suitable initial guess. As the initial guess for the numerical energy minimization we used the first few terms of the Fourier series subjected to the corresponding symmetry. Similar expressions were used in the search for nuclear Skyrme crystals [8],

$$f_2 = \sum_{a,b,c} \alpha_{abc} \sin\left(\frac{2\pi ax}{\lambda_x}\right) \cos\left(\frac{2\pi by}{\lambda_y}\right) \cos\left(\frac{2\pi cz}{\lambda_z}\right),$$

$$f_1 = \sum_{a,b,c} \beta_{abc} \cos\left(\frac{2\pi ax}{\lambda_x}\right) \cos\left(\frac{2\pi by}{\lambda_y}\right) \cos\left(\frac{2\pi cz}{\lambda_z}\right),$$

and f_3 and f_4 were found from f_2 by symmetry transformations. For example, for the st crystal we used (for brevity we assume $\lambda_i = 2\pi$)

$$f_2 = \sin x, \quad f_3 = \sin y, \quad f_4 = \sin z, \\ f_1 = \cos x \cos y \cos z$$

and for the bct crystal (chains)

$$f_2 = \sin x \cos y, \quad f_3 = \sin y \cos z, \quad f_4 = \sin z \cos x, \\ f_1 = c(\cos 2x + \cos 2y + \cos 2z) \\ + (1 - 3c) \cos 2x \cos 2y \cos 2z,$$

with $c \simeq 0.3$.

-
- [1] L. Onsager, *Nuovo Cimento* **6**, 279 (1949).
[2] R. P. Feynman, *Prog. Low Temp. Phys.* **1**, 17 (1955).
[3] A. A. Abrikosov, *Zh. Eksp. Teor. Fiz.* **32**, 1442 (1957) [*Sov. Phys. JETP* **5**, 1174 (1957)].
[4] N. Nagaosa and Y. Tokura, *Nat. Nanotechnol.* **8**, 899 (2013).
[5] T. H. R. Skyrme, *Nucl. Phys.* **31**, 556 (1962).
[6] I. Klebanov, *Nucl. Phys. B* **262**, 133 (1985).
[7] A. S. Goldhaber and N. Manton, *Phys. Lett. B* **198**, 231 (1987).
[8] M. Kugler and S. Shtrikman, *Phys. Lett. B* **208**, 491 (1988).
[9] L. Castillejo, P. Jones, A. Jackson, J. Verbaarschot, and A. Jackson, *Nucl. Phys. A* **501**, 801 (1989).
[10] M. Atiyah and P. Sutcliffe, *Milan J. Math.* **71**, 33 (2003).
[11] P. Fulde and R. A. Ferrell, *Phys. Rev.* **135**, A550 (1964).
[12] A. Larkin and Y. N. Ovchinnikov, *J. Exp. Theor. Phys.* **20**, 762 (1965).
[13] J. A. Bowers and K. Rajagopal, *Phys. Rev. D* **66**, 065002 (2002).
[14] L. Radzihovsky and D. E. Sheehy, *Rep. Prog. Phys.* **73**, 076501 (2010).
[15] Y. Matsuda and H. Shimahara, *J. Phys. Soc. Jpn.* **76**, 1 (2007).
[16] A. L. Gaunt, T. F. Schmidutz, I. Gotlibovych, R. P. Smith, and Z. Hadzibabic, *Phys. Rev. Lett.* **110**, 200406 (2013).
[17] S. J. Garratt, C. Eigen, J. Zhang, P. Turzák, R. Lopes, R. P. Smith, Z. Hadzibabic, and N. Navon, *Phys. Rev. A* **99**, 021601(R) (2019).
[18] B. Mukherjee, Z. Yan, P. B. Patel, Z. Hadzibabic, T. Yefsah, J. Struck, and M. W. Zwierlein, *Phys. Rev. Lett.* **118**, 123401 (2017).
[19] M. Barkman, A. Samoilenka, and E. Babaev, *Phys. Rev. Lett.* **122**, 165302 (2019).
[20] A. Samoilenka, M. Barkman, A. Benfenati, and E. Babaev, [arXiv:1905.03774](https://arxiv.org/abs/1905.03774).
[21] L. Radzihovsky, *Phys. Rev. A* **84**, 023611 (2011).
[22] M. Barkman, A. A. Zyuzin, and E. Babaev, *Phys. Rev. B* **99**, 220508(R) (2019).
[23] D. C. Wright and N. D. Mermin, *Rev. Mod. Phys.* **61**, 385 (1989).
[24] W. V. Liu and F. Wilczek, *Phys. Rev. Lett.* **90**, 047002 (2003).
[25] G. Sarma, *J. Phys. Chem. Solids* **24**, 1029 (1963).
[26] R. Casalbuoni and G. Nardulli, *Rev. Mod. Phys.* **76**, 263 (2004).
[27] M. Jag, M. Cetina, R. S. Lous, R. Grimm, J. Levinsen, and D. S. Petrov, *Phys. Rev. A* **94**, 062706 (2016).
[28] D. Naik, A. Trenkwalder, C. Kohstall, F. Spiegelhalter, M. Zaccanti, G. Hendl, F. Schreck, R. Grimm, T. Hanna, and P. Julienne, *Eur. Phys. J. D* **65**, 55 (2011).
[29] C. Ravensbergen, E. Soave, V. Corre, M. Kreyer, B. Huang, E. Kirilov, and R. Grimm, [arXiv:1909.03424](https://arxiv.org/abs/1909.03424).
[30] X.-L. Qi, E. Witten, and S.-C. Zhang, *Phys. Rev. B* **87**, 134519 (2013).
[31] W. Lee, A. H. Gheorghe, K. Tiurev, T. Ollikainen, M. Möttönen, and D. S. Hall, *Sci. Adv.* **4**, eaao3820 (2018).
[32] Y. Shin, C. H. Schunck, A. Schirotzek, and W. Ketterle, *Phys. Rev. Lett.* **99**, 090403 (2007).
[33] A. Schirotzek, Y.-i. Shin, C. H. Schunck, and W. Ketterle, *Phys. Rev. Lett.* **101**, 140403 (2008).
[34] I. E. Dzyaloshinskii, *Zh. Eksp. Teor. Fiz.* **47**, 992 (1964) [*Sov. Phys. JETP* **20**, 665 (1964)].
[35] Y. Togawa, T. Koyama, K. Takayanagi, S. Mori, Y. Kousaka, J. Akimitsu, S. Nishihara, K. Inoue, A. Ovchinnikov, and J.-i. Kishine, *Phys. Rev. Lett.* **108**, 107202 (2012).